Article
http://justc.ustc.edu.cn Received: March 06, 2025; Accepted: May 23, 2025

Average diffusion of mean–variance from a network perspective: Evidence from the Chinese stock market

Xueli Lu, Renhao Zou ✉, and Hanchao Yang

Department of Statistics and Finance, School of Management, University of Science and Technology of China, Hefei 230026, China

✉Correspondence: Renhao Zou, E-mail: zourh@mail.ustc.edu.cn

Graphical abstract

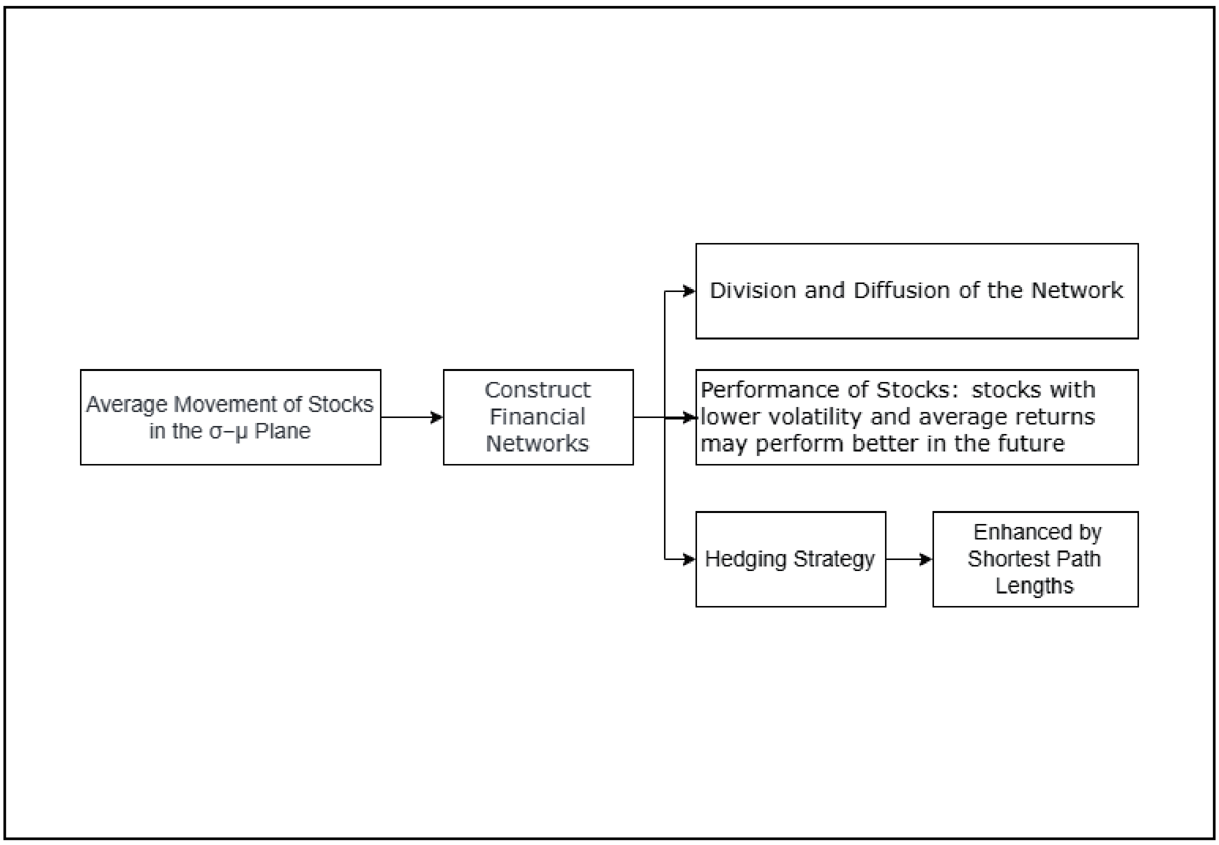

Exploring the stochastic nature of stock movements in the $\sigma-\mu$ plane and revealing optimal hedging strategies through financial networks.

Public summary

■ Investigate average movements in the σ–μ plane using a novel network-based approach.

■ Apply Fisher information distance to construct and partition financial networks.

■ Reveal the stochastic transitions of stocks between network blocks, explaining the failure of MV optimal portfolios.

■ Empirical analysis on Chinese stocks shows that low-volatility, low-return stocks yield better performance in monthly long strategies.

Citation: Lu X L, Zou R H, Yang H C. Average diffusion of mean–variance from a network perspective: Evidence from the Chinese stock market. *JUSTC*, **2025**, 55(0): . CSTR: 32290.14.JUSTC-2025-0029. DOI: 10.52396/JUSTC-2025-0029

JUSTC

Article

http://justc.ustc.edu.cn

Received: March 06, 2025; Accepted: May 23, 2025

Average diffusion of mean–variance from a network perspective: Evidence from the Chinese stock market

Xueli Lu, Renhao Zou ✉, and Hanchao Yang

Department of Statistics and Finance, School of Management, University of Science and Technology of China, Hefei 230026, China

✉Correspondence: Renhao Zou, E-mail: zourh@mail.ustc.edu.cn

Cite This: *JUSTC*, **2025**, 55(X): (7pp)

Read Online

Abstract: This paper investigates the movement of stocks in the $\sigma-\mu$ plane from a mean perspective by constructing financial networks. The variation in diffusion entropy reveals that the network system tends to exhibit increasing stochasticity over time, which may provide a theoretical explanation for the failure of the mean–variance optimal portfolio. The results show that stocks with lower volatility and lower average returns may perform better in the future. Moreover, we propose a hedging strategy and enhance its performance by assigning portfolio weights based on the shortest path lengths from nodes to the barycenter.

Keywords: financial network; minimum spanning tree; entropy; hedging strategy; Chinese stock market

CLC number: F830.91 **Document code:** A

2020 Mathematics Subject Classification: 62P20

1 Introduction

The mean–variance (MV) framework, proposed by Markowitz[1], has received widespread adoption in portfolio optimization[2–4]. However, MV optimization often fails to provide optimal results across various scenarios, which is known as Markowitz optimization enigma[5]. MV portfolio weights exhibit high sensitivity to changes in mean values[6], and even minor deviations in the estimates of mean or variance values can lead to markedly different solutions for MV optimal portfolios[7]. The frequent failure of MV optimization stems from the inability to confidently distinguish between mean returns and variances[8]. Thus, the essence of the MV framework lies in accurately estimating the expected means and variances of asset returns, which means positioning the assets' future location within the $\sigma-\mu$ plane. In efforts to alleviate the impact of errors in mean and variance estimation, numerous scholars have endeavored. Notable methodologies include Bayesian-based portfolios[9–11], global minimum variance portfolios[12, 13], and robust portfolio optimization[14, 15]. These methods focus on estimating individual assets. However, as the number of assets increases, the cumulative effect of errors may amplify their overall impact. Therefore, we are motivated to examine movements in the $\sigma-\mu$ plane from the standpoint of asset groups.

In this paper, we utilize mean-field theory[16] and financial networks to explore the average movements of stocks sharing similar return-volatility characteristics in the Chinese stock market. The use of networks facilitates the examination of interconnections among different stocks. First, we employ the correlation-based method to construct the networks. Following Khashanah and Yang[17], we assess the correlation between stocks via the Fisher information distance. Under some assumptions, the correlation between two stocks can be calculated via the mean and standard deviation of their returns, making it suitable for our objective of analyzing stock movements in the $\sigma-\mu$ plane. The minimum spanning tree (MST)[18–20] pruning algorithm is then used to eliminate nonessential edges because of its simplicity, robustness, and capacity to highlight the most critical relationships among the stocks. Second, we propose a method to partition the stocks into several blocks. Unlike community detection methods[21–24], our proposed approach aggregates nodes on the basis of the topological structure of the network, as well as the characteristics of stock returns and volatilities. Third, we examine the transition process of stock nodes between blocks. During this process, an increasing entropy effect is observed. Finally, hedging strategies are identified on the basis of the differences in returns between blocks, and weighted portfolio optimization with the shortest path length (SPL) is employed to achieve higher investment returns.

The main contributions of this work are outlined as follows. First, we investigate the average movements in the $\sigma-\mu$ plane from a network perspective, enriching the methodologies for studying the MV framework. Second, we utilize the Fisher information distance for network construction and partition, extending the work of Khashanah & Yang[17]. Third, we discover that the movement of stocks between different blocks in the $\sigma-\mu$ plane is stochastic, which may explain the failure of MV optimal portfolios. Fourth, the empirical results suggest that on the basis of block partitioning and transition analysis in the $\sigma-\mu$ plane for Chinese stocks, stocks with lower volatility and lower average returns are better choices for monthly long strategies, achieving higher annualized returns and Sharpe ratios, as well as lower maximum drawdowns.

The remaining structure of this paper is outlined as follows. Section 2 describes the methodology. Section 3 presents the data and some empirical results. Section 4 introduces the hedging strategies and their performance measures. And Section 5 concludes the paper.

2 Methodology

2.1 Construction of the network

The set of stocks is used to represent the set of vertices in the network. Following Khashanah and Yang[17], we employ the Fisher information distance to measure the correlations between stocks. Like measures such as Kullback Leibler, Bregman, and Burbea-Rao, the Fisher information distance serves as a method for measuring the dissimilarity between probability distributions[25]. Intuitively, the Fisher information distance quantifies how easily two probability distributions can be distinguished on the basis of their parameters, making it particularly useful for analyzing differences in the statistical properties of stock returns. It can thus serve as a proxy for the "distance" or dissimilarity between stocks in correlation analysis. In the empirical study, we assume that the distribution of stock returns follows a Gaussian distribution①, and the Fisher information distance between stocks can be calculated with the means and standard deviations of their returns.

Let $V=\{1,2,\cdots,n\}$ denotes the set of stocks, and $R_{i,t}$ is the logarithmic return of stock i on day t. The mean and standard deviation of the logarithmic returns of stock i at time t over the past year (including 252 trading days) are given by

$$\mu_{i,t}=\frac{1}{252}\sum_{k=0}^{251}R_{i,t-k}, \tag{1}$$

$$\sigma_{i,t}=\sqrt{\frac{1}{251}\sum_{k=0}^{251}(R_{i,t-k}-\mu_{i,t})^2}. \tag{2}$$

Under the Gaussian assumption, the Fisher information distance between nodes i and j can be calculated as follows:

$$d_{ij}^{t}=\sqrt{2}\ln\left(\frac{\mathcal{F}(\mu_{i,t},\sigma_{i,t},\mu_{j,t},\sigma_{j,t})+(\mu_{i,t}-\mu_{j,t})^2+2\left(\sigma_{i,t}^2+\sigma_{j,t}^2\right)}{4\sigma_{i,t}\sigma_{j,t}}\right), \tag{3}$$

where

$$\mathcal{F}(\mu_{i,t},\sigma_{i,t},\mu_{j,t},\sigma_{j,t})=\sqrt{\left[(\mu_{i,t}-\mu_{j,t})^2+2(\sigma_{i,t}-\sigma_{j,t})^2\right]\left[(\mu_{i,t}-\mu_{j,t})^2+2(\sigma_{i,t}+\sigma_{j,t})^2\right]}.$$

A fully connected network can be constructed with distances, on the basis of which Kruskal's algorithm[27] is then employed to generate the MST of the fully connected network.

2.2 Network division rules

For stocks close in the $\sigma-\mu$ plane that share similar return-volatility characteristics, we tend to group these stocks into the same block. In the $\mu-\sigma$ plane, we establish a Cartesian coordinate system with the barycenter of the network as the origin. Specifically, the barycenter is computed as the arithmetic mean of the σ and μ values across all stocks, representing the average position of the nodes in the plane. The two coordinate axes naturally divide the entire plane into four quadrants, and correspondingly, the nodes in the network are also divided into four blocks. Each block, which is aligned with the respective quadrant that it occupies, is labeled as 1, 2, 3, or 4. Subdivision is then based on the SPLs from each node to the barycenter. Taking block 1 as an example, the median SPL can be used as a threshold to divide block 1 into two subblocks denoted as 1 and 5, where block 1 represents the nodes closer to the origin. Consequently, we divide the entire network into eight blocks, with blocks 1, 2, 3, and 4 representing the blocks closer to the barycenter in each quadrant. The visualization of this division is shown in Fig. 1. Similarly, the network can be further subdivided into more blocks, such as 12, 16 and 20. Further subdivision into additional blocks, such as 12, 16 and 20, follows the same rules, with larger numerical labels assigned to blocks farther from the barycenter within each quadrant.

2.3 Block diffusion entropy

The positions of stocks in the $\sigma-\mu$ plane are continuously changing over time. Our interest lies in examining the positions of stocks in the $\sigma-\mu$ plane after a certain time interval. As mentioned before, an analysis is conducted from the perspective of mean-field theory to study the average movement of stocks within each block. One stock may be assigned to different blocks in the network at different times. In other words, stocks in one block may transfer to other blocks in the new network after a period of time. To characterize the degree of dispersion of the transitions of nodes within each block, we introduce the block diffusion entropy, which can be computed with Eq. (4), where $P_{I,J}^{t,\triangle t}$ represents the probability that nodes within block I on day t are located in block J after a time interval $\triangle t$, and k is the number of blocks.

$$En_I^{t,\triangle t}=-\sum_{J=1}^{k}P_{I,J}^{t,\triangle t}\log P_{I,J}^{t,\triangle t}. \tag{4}$$

The value of $En_I^{t,\triangle t}$ reflects the degree of nondeterminacy in the diffusion of block I from t to $t+\triangle t$. A higher value indicates a greater dispersion of stocks within this block at $t+\triangle t$ across different blocks. $En_I^{\triangle t}$ denotes the mean of $En_I^{t,\triangle t}$ over the time period, which can be calculated as follows:

$$En_I^{\triangle t}=\frac{\sum_{i=1}^{m}En_I^{t_i,\triangle t}}{m}. \tag{5}$$

$En_I^{\triangle t}$ provides an average measure of the dispersion of stocks within block I after a time interval $\triangle t$.

3 Data and empirical results

① Although the distributions of stock returns are generally non-Gaussian[26], our assumption focuses on the overall characteristics of stock returns, such as the means and variances, rather than the specific distributional form of the returns.

CSTR: 32290.14.JUSTC-2025-0029
DOI: 10.52396/JUSTC-2025-0029
JUSTC, **2025**, 55(X):

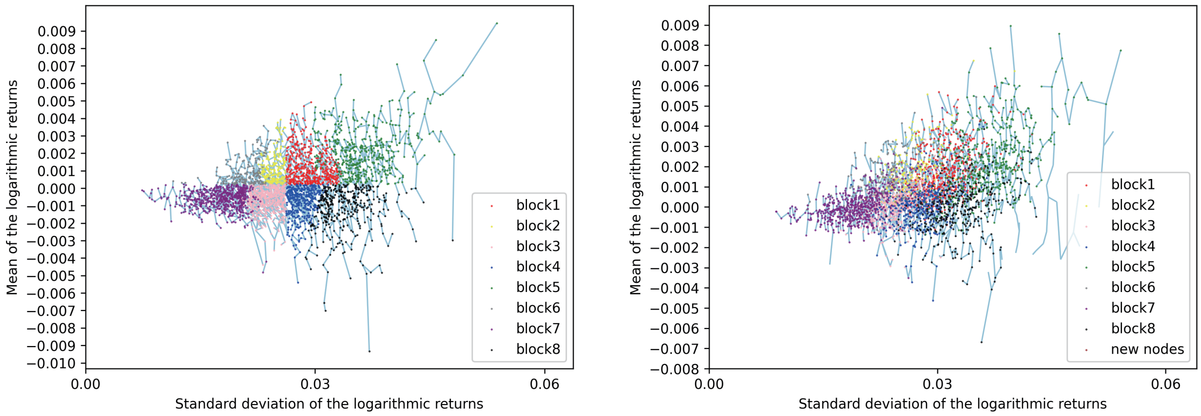

Fig. 1. Visualization result. Left panel: The network on May 18, 2020. Right panel: The network 60 trading days later, with the same colors denoting the same stock nodes on May 18, 2020.

3.1 Data

All Chinese A-share stocks are selected as our sample. Daily stock price and market capitalization data are obtained from the China Stock Market and Accounting Research (CSMAR) database. The sample period spans from January 4, 2005 to February 27, 2024, including the time of the financial crisis in 2008 and the COVID-19 pandemic in 2020, making this period comprehensive. The sample consists of a total of 5388 stocks with 13055339 daily observations. We calculate the logarithmic returns of these stocks and update the financial network every 20 trading days. Notably, to ensure that the stock nodes in the network have sufficient liquidity and lower risk of delisting, we construct the network by excluding the bottom 5% of stocks on the basis of their market capitalization at each timestamp.

3.2 The division and diffusion of the network

We introduce a visualization approach for our network. Typically, in network visualization, the spatial arrangement of nodes does not impact the network structure, allowing for flexible node distributions in visualizations. Considering that Fisher information distances define the distances between nodes, expressed as the means and standard deviations of logarithmic returns under the Gaussian assumption, we utilize the $\sigma-\mu$ plane for our network visualization. Specifically, the coordinates of node i at time t are set as $(\sigma_{i,t}, \mu_{i,t})$ in the $\sigma-\mu$ plane. Consequently, the outcome of network partitioning can be illustrated in the $\sigma-\mu$ plane. Fig. 1 illustrates the financial networks on May 18, 2020 and 60 trading days later when dividing the network into eight blocks. As shown in the left panel, most edges connect nodes within the same block, with only a small fraction linking to nodes in different blocks. Moreover, nodes within the same block are densely clustered in the $\sigma-\mu$ plane, indicating their relatively similar average return-volatility characteristics.

The right panel illustrates the financial network 60 trading days after May 18, 2020. A number of nodes have undergone changes in their block assignments, attributed to the movements of nodes in the $\sigma-\mu$ plane. Owing to ongoing stock listings and delistings in the market, the nodes included in the financial network at each timestamp may vary. Taking this into consideration, when characterizing the average movement patterns of stocks in the network, we introduce a new block named “out”. This block consists of nodes that do not exist in the new network. Tables 1–3 illustrate the average transition probability of stocks within each block at intervals of 20, 200, and 500 trading days, respectively, where the entry in the Ith row and Jth column represents the average probability of block I transitioning to block J after the trading days. We observe that within short time intervals, nodes in each block tend to remain in their respective blocks with high probability. However, over longer time intervals, the new distribution of nodes within each block becomes more dispersed.

Fig. 2 illustrates the variation in the block diffusion en-

Table 1. The average transition probability matrix within blocks over 20 trading days.

	1	2	3	4	5	6	7	8	Out
1	**0.6132**	0.0593	0.0277	0.1256	0.1294	0.0016	0.0003	0.0351	0.0077
2	0.1314	**0.5699**	0.1602	0.0170	0.0046	0.0866	0.0227	0.0005	0.0071
3	0.0298	0.1566	**0.6182**	0.0603	0.0005	0.0204	0.1035	0.0026	0.0079
4	0.1820	0.0219	0.1464	**0.5370**	0.0123	0.0004	0.0025	0.0876	0.0097
5	0.0887	0.0015	0.0003	0.0119	**0.7727**	0.0006	0.0003	0.1185	0.0054
6	0.0096	0.1202	0.0313	0.0006	0.0014	**0.6677**	0.1597	0.0001	0.0094
7	0.0018	0.0305	0.0754	0.0024	0.0005	0.1670	**0.7146**	0.0004	0.0075
8	0.0564	0.0009	0.0093	0.1389	0.1252	0.0000	0.0011	**0.6556**	0.0127

The entry in the Ith row and Jth column represents the average probability of block I transitioning to block J after the trading days. The bold fonts represent the maximum value among the transition probabilities of one block.

CSTR: 32290.14.JUSTC-2025-0029
DOI: 10.52396/JUSTC-2025-0029
JUSTC, **2025**, 55(X):

Table 2. The average transition probability matrix within blocks over 200 trading days.

	1	2	3	4	5	6	7	8	Out
1	**0.2067**	0.1147	0.1483	0.1223	0.1916	0.0483	0.0651	0.0843	0.0186
2	**0.1868**	0.1749	0.1465	0.0686	0.1139	0.1290	0.1252	0.0366	0.0186
3	0.1537	0.1614	**0.1829**	0.0795	0.0881	0.1039	0.1729	0.0359	0.0218
4	0.1814	0.1133	**0.1825**	0.1314	0.1390	0.0453	0.0973	0.0820	0.0277
5	0.1448	0.0473	0.0894	0.1346	**0.2928**	0.0199	0.0266	0.2250	0.0196
6	0.1138	0.1432	0.0857	0.0333	0.0688	**0.2902**	0.2131	0.0231	0.0289
7	0.0864	0.1317	0.1080	0.0349	0.0460	0.2619	**0.2903**	0.0194	0.0215
8	0.1469	0.0565	0.1373	0.1629	0.1889	0.0206	0.0526	**0.1928**	0.0416

The table notes are the same as those in Table 1.

Table 3. Average transition probability matrix within blocks over a span of 500 trading days.

	1	2	3	4	5	6	7	8	Out
1	**0.1601**	0.1203	0.1462	0.1087	0.1412	0.0892	0.1150	0.0903	0.0291
2	0.1432	0.1355	0.1414	0.0843	0.1096	0.1354	**0.1560**	0.0663	0.0283
3	**0.1636**	0.1369	0.1318	0.0785	0.1378	0.1184	0.1346	0.0644	0.0340
4	0.1720	0.1143	0.1339	0.1001	**0.1721**	0.0793	0.1000	0.0874	0.0410
5	0.1546	0.0908	0.1458	0.1312	**0.1654**	0.0552	0.0858	0.1376	0.0336
6	0.1127	0.1206	0.1138	0.0638	0.0744	**0.2133**	0.2114	0.0524	0.0377
7	0.1212	0.1285	0.1107	0.0570	0.0898	**0.2152**	0.2046	0.0411	0.0318
8	0.1646	0.0928	0.1257	0.1117	**0.1909**	0.0587	0.0737	0.1142	0.0676

The table notes are the same as those in Table 1.

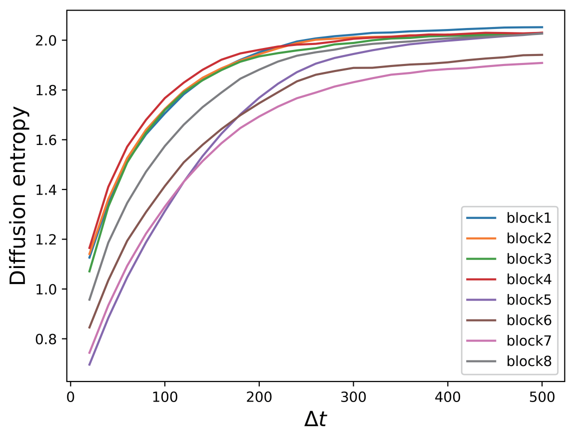

Fig. 2. The variation in diffusion entropy.

tropy, where the vertical axis corresponds to the average value of block diffusion entropies at different timestamps. We observe the presence of the entropy-increasing effect in the transition process. The diffusion entropy in each block converges to a common value over time, indicating a tendency toward randomness in block diffusion. This can explain the failure of MV optimal portfolios to some extent, as stocks located on the efficient frontier have a lower probability of staying there after a period of time. Moreover, for short time intervals, blocks farther away from the barycenter exhibit smaller diffusion entropies, suggesting higher determinism and suitability for constructing investment strategies.This occurs because stocks in blocks farther from the barycenter typically exhibit lower volatility, resulting in more predictable and less random behavior over time. As a result, these stocks show smaller diffusion entropy, indicating fewer transitions between blocks, which can be beneficial for constructing stable investment strategies.

4 Hedging strategies

4.1 Performance of blocks

We continue to explore investment strategies based on eight blocks. We first examine the return-volatility characteristics of the stocks within each block. Considering the changes of stocks within each block, updates are made every 20 trading days. Employing a simple equal-weight method, the average returns of stocks within each block for the subsequent 20 trading days are calculated. After 20 trading days, using the new network, we identify the new stocks and compute the future returns via the same method. The results are presented in Table 4. We find that in blocks with comparable volatility levels in the past, the blocks with lower average returns performed better. This finding is consistent with the observation that reversal strategies are profitable for monthly investment horizons in the Chinese stock market[28]. Moreover, in blocks

CSTR: 32290.14.JUSTC-2025-0029
DOI: 10.52396/JUSTC-2025-0029
JUSTC, **2025**, 55(X):

Table 4. Performance of each block.

Block	Annualized return	Sharpe ratio	Maximum retracement
1	14.36%	0.5874	−73.29%
2	16.15%	0.6742	−71.65%
3	21.88%	0.8184	−66.75%[a]
4	18.67%	0.6969	−69.61%
5	4.68%[b]	0.3059[b]	−82.10%[b]
6	17.19%	0.8151	−67.32%
7	23.92%[a]	0.9725[a]	−66.83%
8	11.58%	0.4957	−71.86%

Superscript a indicates the best performance, whereas superscript b indicates the worst performance among the blocks.

Table 5. Performance under different rebalancing frequencies.

Rebalancing intervals	Annualized return	Sharpe ratio	Maximum retracement
5	−2.77%	-0.3101	−49.11%
10	2.03%	0.2918	−26.40%
20	4.59%	0.6159	−16.18%
40	**6.19%**	**0.8359**	**−14.83%**
60	5.66%	0.7705	−15.57%
120	5.06%	0.6772	−24.79%
240	3.19%	0.4423	−24.79%

The bold font indicates the best performance among the different rebalancing intervals.

with comparable average returns in the past, the performance of blocks with lower volatility is better, in line with the phenomenon known as the low-volatility anomaly[29]. The low-volatility anomaly may arise from the tendency of low-volatility stocks to have less risk, making them more attractive to risk-averse investors. Furthermore, these stocks may experience less dramatic price fluctuations, leading to more stable returns over time. Some theories also suggest that investors may irrationally overvalue high-volatility stocks, leading to higher returns for low-volatility stocks in the long run. The managerial implication of this for investors is that stocks with lower volatility and lower average returns may be preferable choices for monthly long strategies.

4.2 Construction of hedging strategies

When constructing hedging strategies, we start with a simple equal-weighted situation, where long and short positions in stocks are equally weighted, and the allocation for both long and short positions is set at a 1 : 1 ratio. Owing the greater determinism of the blocks located farther from the barycenter after short time intervals and the large difference between the performance measures of blocks 5 and block 7, we consider a long position in stocks within block 7 and a short position in stocks within block 5. The total transaction costs are assumed to be 0.2% including commissions, stamp duties, and other expenses.This value is chosen on the basis of average transaction costs in the Chinese stock market, which typically range between 0.1% and 0.3%, depending on the broker and the type of transaction. The assumption of 0.2% provides a reasonable estimate of the costs associated with executing the hedge strategy.

Table 5 shows the performance of the hedging strategy under different rebalancing frequencies. Notably, we attempt to rebalance every 5 and 10 trading days, so we need to update the network at a higher frequency. The annualized returns and Sharpe ratios both increase initially and then decrease with decreasing rebalancing frequency, reaching their maximum values when the rebalancing frequency is 40 trading days. Additionally, the maximum drawdown associated with this trading frequency is also the smallest. Therefore, the best trading frequency for this hedging strategy is 40 trading days. The strategies presented later in this paper all use a rebalancing frequency of 40 trading days. The strategy incurs losses notably when the rebalancing frequency is set to 5 trading days. This is attributed to the excessively frequent trading, which results in the inability of the long-short returns differential to cover the transaction costs.

Huang et al.[19] reported a positive correlation between the normalized tree length and market returns. Inspired by this finding, we attempt to incorporate the SPLs from each node to the barycenter into the aforementioned strategy. We explore this approach from the following three perspectives:

(i) Maintaining a 1 : 1 weighting for long and short positions, applying weights individually to both long and short stocks, with the weight of each stock positively correlated with its SPL to the barycenter. Specifically, the weight assigned to the stock i in the long portfolio is defined as

$$w_i = \frac{SPL_i}{\sum\limits_{j\in\mathrm{Long}} SPL_j},$$

where SPL_i represents the SPL of stock i to the barycenter, and "Long" denotes the set of all stocks in the long position. The same is true for the stocks in the short portfolio.

(ii) Maintaining equal weights among stocks within both the long and short positions, we assign a weight of

$$w_{\mathrm{Long}} = \frac{SPL_{\mathrm{Long}}}{SPL_{\mathrm{Long}} + SPL_{\mathrm{Short}}}$$

to the long positions and $w_{\mathrm{Short}} = 1 - w_{\mathrm{Long}}$ to the short positions. Here, SPL_{Long} and SPL_{Short} represent the average SPLs from all stocks in the long and short positions to the barycenter.

(iii) The two weighting methods mentioned above are applied simultaneously.

The performance measures are detailed in Table 6, and the corresponding return curves are presented in Fig. 3, where weighting method 0 denotes the simple equal-weighting approach. The results indicate that both weighting methods exhibit significant improvements over the simple equal-weighted strategy. Despite the increase in maximum drawdown, the combined method has increased the annualized return by 2.49% and improved the Sharpe ratio by approximately 0.2. In comparison, the maximum drawdown has only increased by 0.52%, which is almost negligible.

Finally, employing weighting method 3, we compare the

CSTR: 32290.14.JUSTC-2025-0029
DOI: 10.52396/JUSTC-2025-0029
JUSTC, **2025**, 55(X):

Table 6. Performance of strategies with different weighting methods.

Weighting method	Annualized return	Sharpe ratio	Maximum retracement
0	6.19%	0.8359	**−14.83%**
1	7.60%	0.8901	−15.22%
2	7.32%	0.9921	−14.93%
3	**8.68%**	**1.0393**	−15.35%

The bold font indicates the best performance among the different weighting methods. Method 0 represents the simple equal-weighting strategy. Method 1 applies SPL-based weighting within each side. Method 2 assigns equal weights within each side but adjusts overall portfolio weights on the basis of average SPLs. And Method 3 combines both methods. The detailed formulas are provided in the main text.

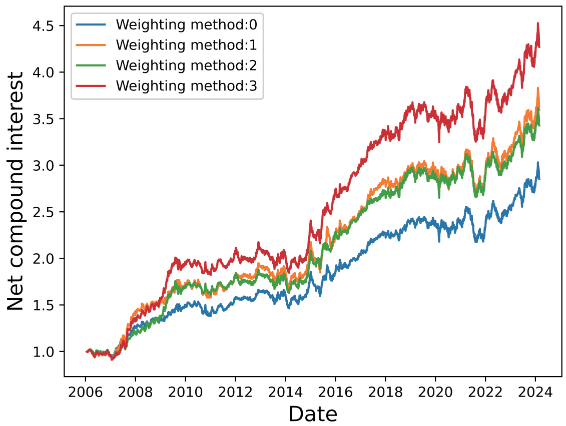

Fig. 3. Net compound interest curve. The weighting methods 0, 1, 2, and 3 are defined consistently with those in Table 6.

impacts of different block numbers on the strategy outcomes. Similar to the case with 8 blocks, we also choose the stocks within the blocks with the largest SPLs away from the barycenter. We long the stocks within the block with low volatility and low returns and short those with high volatility and high returns. Taking the example of 16 blocks, we choose to lengthen the stocks within block 15 and shorten those within block 13. The results are illustrated in Table 7. As the number of blocks increases, the annualized return, Sharpe ratio and maximum drawdown clearly exhibit increasing trends, except for the cases where the number of blocks is 4 and 32. As the number of blocks increases, the division of the network becomes more refined, leading to greater disparities among the stocks in the long and short portfolios. This refinement contributes to higher returns. At the same time, fewer stocks are included in the portfolios, resulting in higher risks. In the case of 32 blocks, the long portfolio consists of a minimum of only 10 stocks. For this reason, we do not divide the network into more blocks.

5 Conclusions

In this paper, we construct financial networks to study the average movement of stocks in the $\sigma-\mu$ plane. The Fisher information distance and Kruskal's algorithm are used in the construction of the network. On the basis of the return-volatility characteristics of stocks and the topological properties of stock nodes in the network, we partition the financial network into several blocks and investigate the average movement patterns of each block. In this process, we observe the entropy-increasing effect during the transition of blocks, indicating a tendency toward randomness in the block diffusion. Additionally, our research reveals that stocks with low-return and low-volatility characteristics tend to perform better in the future, leading to the proposal of hedging strategies. We further enhance the performance of our strategy by assigning weights to the portfolios in our strategy using the SPLs from stock nodes to the barycenter. The impact of the number of partitions on the strategy results is also considered, with more refined division yielding higher returns and risks.

Table 7. Performance of strategies with different numbers of blocks.

Number of blocks	Annualized return	Sharpe ratio	Maximum retracement
4	6.90%	0.9465	−17.04%
8	8.68%	1.0393	**−15.35%**
12	10.26%	1.1083	−16.34%
16	11.20%	1.1182	−17.24%
20	12.29%	1.1466	−17.88%
24	13.09%	1.1563	−18.22%
28	**13.66%**	**1.1565**	−18.33%
32	13.47%	1.0992	−19.06%

The bold fonts indicate the best performance among different numbers of blocks.

Acknowledgements

The authors would like to thank Professor Shuguang Zhang for his valuable guidance throughout this research. We also thank Dr. Zixin Liu and Dr. Zhipeng He for their helpful discussions and support.

Conflict of interest

The authors declare that they have no conflict of interest.

Biographies

Xueli Lu is a Master's student in Statistics at the School of Management, University of Science and Technology of China. His research mainly focuses on financial data analysis.

Renhao Zou is a Ph.D. candidate at the University of Science and Technology of China. His research mainly focuses on financial econometrics, machine learning in finance, and asset pricing.

References

[1] Markowitz H M. Portfolio selection. *Journal of Finance*, **1952**, *7* (1): 77–91.
[2] Zhang Y, Li X, Guo S. Portfolio selection problems with Markowitz's mean–variance framework: A review of literature. *Fuzzy Optimization and Decision Making*, **2018**, *17*: 125–158.
[3] Dai M, Jin H, Kou S, et al. A dynamic mean–variance analysis for log returns. *Management Science*, **2021**, *67* (2): 1093–1108.

CSTR: 32290.14.JUSTC-2025-0029
DOI: 10.52396/JUSTC-2025-0029
JUSTC, **2025**, 55(X):

[4] Butler A, Kwon R H. Integrating prediction in mean–variance portfolio optimization. *Quantitative Finance*, **2023**, *23* (3): 429–452.
[5] Michaud R O. The Markowitz optimization enigma: Is 'optimized' optimal? *Financial Analysts Journal*, **1989**, *45* (1): 31–42.
[6] Best M J, Grauer R R. On the sensitivity of mean–variance efficient portfolios to changes in asset means: some analytical and computational results. *Review of Financial Studies*, **1991**, *4* (2): 315–342.
[7] Chopra V K. Improving optimization. *Journal of Investing*, **1993**, *2* (3): 51–59.
[8] Mynbayeva E, Lamb J D, Zhao Y. Why estimation alone causes Markowitz portfolio selection to fail and what we might do about it. *European Journal of Operational Research*, **2022**, *301* (2): 694–707.
[9] Tu J, Zhou G. Incorporating economic objectives into Bayesian priors: Portfolio choice under parameter uncertainty. *Journal of Financial and Quantitative Analysis*, **2010**, *45* (4): 959–986.
[10] Jorion P. Bayes-Stein estimation for portfolio analysis. *Journal of Financial and Quantitative Analysis*, **1986**, *21* (3): 279–292.
[11] Huang X, Han W, Newton D, et al. The diversification benefits of cryptocurrency asset categories and estimation risk: pre and post Covid-19. *European Journal of Finance*, **2023**, *29* (7): 800–825.
[12] Bodnar T, Mazur S, Okhrin Y. Bayesian estimation of the global minimum variance portfolio. *European Journal of Operational Research*, **2017**, *256* (1): 292–307.
[13] Reh L, Krüger F, Liesenfeld R. Predicting the global minimum variance portfolio. *Journal of Business & Economic Statistics*, **2023**, *41* (2): 440–452.
[14] Van Parys B P G, Esfahani P M, Kuhn D. From data to decisions: Distributionally robust optimization is optimal. *Management Science*, **2021**, *67* (6): 3387–3402.
[15] Sehgal R, Jagadesh P. Data-driven robust portfolio optimization with semi mean absolute deviation via support vector clustering. *Expert Systems with Applications*, **2023**, *224*: 120000.
[16] Barabási A-L, Albert R, Jeong H. Mean-field theory for scale-free random networks. *Physica A: Statistical Mechanics and its Applications*, **1999**, *272* (1-2): 173–187.
[17] Khashanah K, Yang H. Evolutionary systemic risk: Fisher information flow metric in financial network dynamics. *Physica A: Statistical Mechanics and its Applications*, **2016**, *445*: 318–327.
[18] Mantegna R N. Hierarchical structure in financial markets. *European Physical Journal B: Condensed Matter and Complex Systems*, **1999**, *11*: 193–197.
[19] Huang C, Zhao X, Su R, et al. Dynamic network topology and market performance: A case of the Chinese stock market. *International Journal of Finance & Economics*, **2022**, *27* (2): 1962–1978.
[20] Rehman M U, Ahmad N, Hussain Shahzad S J, et al. Dependence dynamics of stock markets during COVID-19. *Emerging Markets Review*, **2022**, *51*: 100894.
[21] Newman M E J. Modularity and community structure in networks. *Proceedings of the National Academy of Sciences*, **2006**, *103* (23): 8577–8582.
[22] Javed M A, Younis M S, Latif S, et al. Community detection in networks: A multidisciplinary review. *Journal of Network and Computer Applications*, **2018**, *108*: 87–111.
[23] Wang J, Zhang J, Liu B, et al. Fast network community detection with profile-pseudo likelihood methods. *Journal of the American Statistical Association*, **2023**, *118* (542): 1359–1372.
[24] Ding Y, Li Y, Liu G, et al. Stock co-jump networks. *Journal of Econometrics*, **2024**, *239* (2): 105420.
[25] Costa S I R, Santos S A, Strapasson J E. Fisher information distance: A geometrical reading. *Discrete Applied Mathematics*, **2015**, *197*: 59–69.
[26] De Domenico F, Livan G, Montagna G, et al. Modeling and simulation of financial returns under non-Gaussian distributions. *Physica A: Statistical Mechanics and its Applications*, **2023**, *622*: 128886.
[27] Kruskal J B. On the shortest spanning subtree of a graph and the traveling salesman problem. *Proceedings of the American Mathematical Society*, **1956**, *7* (1): 48–50.
[28] Gang J, Qian Z, Xu T. Investment horizons, cash flow news, and the profitability of momentum and reversal strategies in the Chinese stock market. *Economic Modelling*, **2019**, *83*: 364–371.
[29] Baker M, Bradley B, Wurgler J. Benchmarks as limits to arbitrage: Understanding the low-volatility anomaly. *Financial Analysts Journal*, **2011**, *67* (1): 40–54.

CSTR: 32290.14.JUSTC-2025-0029
DOI: 10.52396/JUSTC-2025-0029
JUSTC, **2025**, 55(X):